Frontiers of Environmental Science & Engineering
2025, 19(5): 70 https://doi.org/10.1007/s11783-025-1990-y

RESEARCH ARTICLE

Intermediate and semi-volatility organic compounds (I/SVOCs) emission from Chinese vehicles: volatility distribution, influencing factors, and implication for SOA formation

Yajun Wu[1,#], Peiji Liu[1,#], Yajie Wang[1], Xiaoguo Wang[2], Jing Zhang ✉ [2], Yan Liu[1], Jinsheng Zhang[1], Lin Wu[1], Ting Wang[1], Hongjun Mao[1], Jianfei Peng ✉ [1]

1. Tianjin Key Laboratory of Urban Transport Emission Research, College of Environmental Science and Engineering, Nankai University, Tianjin 300071, China
2. Tianjin Eco-Environmental Monitoring Center, Tianjin 300071, China

HIGHLIGHTS

- I/SVOCs profile and volatility distributions from vehicles were established.
- Stricter emission standards reduced organic emissions but increased I/SVOC fraction.
- Speciation analysis enhanced SOA prediction accuracy compared to GC-MS.

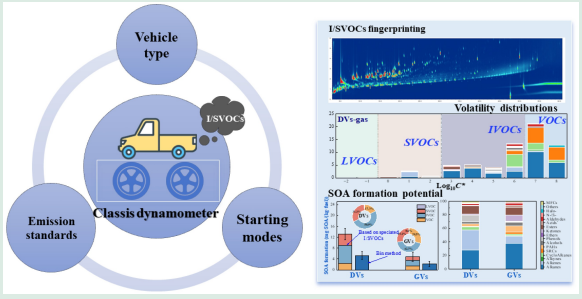

ABSTRACT: Intermediate and semi-volatility organic compounds (I/SVOCs) are crucial precursors for secondary organic aerosols (SOA). Vehicles are major sources of I/SVOCs, yet their emission profiles remain insufficiently characterized. We conducted dynamometer tests on eight in-use gasoline and diesel vehicles (DVs), employing non-targeted analysis with comprehensive two-dimensional gas chromatography coupled with high-resolution mass spectrometry (GC × GC-TOFMS) to investigate vehicular I/SVOC emissions at the molecular level. A total of 438 and 424 compounds were identified and (semi)-quantified in the gas and particle phases, respectively. DVs exhibited higher emission factors (376.7 ± 74.9 mg/(kg·fuel)) compared to gasoline vehicles (GVs) (114.4 ± 42.1 mg/(kg·fuel)) across both phases. Alkanes (29.7%–41.9%), single-ring aromatics (2.6%–29.8%), and cycloalkanes (1.0%–13.1%) were dominant I/SVOCs groups. Oxygenated I/SVOCs were more abundant in particulate phases (40.3%–56.8%) than in gas phases (14.4%–15.3%). Upgrading emission standards reduced organic emissions by 89.2% from China IV to China VI for DVs, particularly in the particle phase. Cold-start conditions resulted in higher I/SVOC emissions (528.4 mg/(kg·fuel)) than hot-starts (224.8 mg/(kg·fuel)) due to reduced combustion efficiency and suboptimal after-treatment performance at low temperatures. Our composition-based SOA estimation method improved SOA predictions by 1.5 and 1.2 times for diesel and GVs, respectively, compared to the traditional bin approach. These findings provide valuable insights into the molecular composition of vehicular I/SVOCs and their environmental impacts.

✉ Corresponding authors. E-mails: zhangjing_gogo@126.com (J. Zhang); pengjianfei@nankai.edu.cn (J. Peng)

# These authors contributed equally to this work.

Article history: Received 11 November 2024, Revised 11 March 2025, Accepted 12 March 2025, Available online 2 April 2025

KEYWORDS: Vehicle emissions, Non-targeted analysis, I/SVOCs, Chemical fingerprinting, SOA formation potential

1 Introduction

Secondary organic aerosol (SOA) significantly contributes to atmospheric fine particulate matter (Peng et al., 2021; Zhao et al., 2024), adversely affecting climate (Shrivastava et al., 2017) and human health (Qiao et al., 2022). Identifying and regulating SOA precursors is essential for improving air quality. Beyond traditional SOA precursors, e.g., volatile organic compounds (VOCs), Robinson et al. (2007) emphasized the importance of Intermediate and semi-volatility organic compounds (I/SVOCs) as key contributors. These compounds, typically defined by effective saturation concentrations (C^*, ranging from 1 to 10^6 μg/m^3) (Lu et al., 2018), have a high potential to generate low-volatility SOA through atmospheric oxidation (Robinson et al., 2007; Presto et al., 2009; Zhao et al., 2014; Li et al., 2024).

Nowadays, our understanding of I/SVOCs remains limited due to significant analytical challenges in identifying and quantifying individual I/SVOCs, resulting in a substantial unresolved complex mixture (UCMs) (Zhao et al., 2014; Zhao et al., 2016; Wu et al., 2023a). Conventional instruments, such as gas chromatography-mass spectrometry (GC-MS), often fail to resolve I/SVOCs at the molecular level, leaving a significant fraction unidentified (80%–90%). Research has shown that UCMs contribute significantly to SOA production (~80%). Zhao et al. (2015) proposed a rough categorization of UCMs into speciated IVOCs based on the retention times of n-alkane, identifying groups such as branched alkanes and cyclic compounds. However, a significant portion remains unspecified (Alam et al., 2019). Given the predominant proportion of UCMs, current I/SVOCs speciation remains rudimentary, lacking essential structural details, such as carbon skeletons and chemically active moieties. This gap in chemical analysis limits the ability to fully understand and estimate SOA contributions. Previous studies (Zhao et al., 2014; Qi et al., 2021; Tang et al., 2021) may have underestimated the contribution of organic compounds to SOA formation, as they quantified only a limited range of homologs. Consequently, comprehensive emission data are essential for accurately depicting atmospheric chemistry and understanding their contributions to SOA formation. Over the past decade, significant efforts have focused on achieving near-complete characterization and quantification of SOA precursors.

Recently, comprehensive two-dimensional gas chromatography (GC × GC) coupled with high-resolution mass spectrometry has improved the ability to separate complex organic compounds. GC × GC is recognized for its enhanced sensitivity, broad selectivity, and high peak capacity, which are achieved through the connection of two capillary columns with complementary stationary phases (Dallüge et al., 2003; An et al., 2021). It has been employed to investigate organics from various sources, including cooking emissions (Song et al., 2023a), biomass coal combustion (Huo et al., 2021a), and vehicle exhausts (He et al., 2022b). Compared to one-dimensional GC, it offers significantly enhanced resolution, effectively reducing UCMs and minimizing coelution (Huo et al., 2021b).

On-road vehicle emissions are a major source of I/SVOCs in urban atmospheres (Qi et al., 2021; Zhao et al., 2022; Wu et al., 2023b). Chassis dynamometer testing is a widely used method for quantifying vehicular emissions (Tang et al., 2021; Zeng et al., 2024). In recent years, China has progressively strengthened emission standards to reduce vehicular emissions. While these standards have effectively reduced total organic emissions, particularly VOCs, significant challenges remain in controlling I/SVOCs (Huang et al., 2024; Zhang et al., 2024b), which play a crucial yet under-regulated role in SOA formation. Although numerous studies have measured individual I/SVOCs (e.g., large n-alkanes and PAHs) based on conventional chromatography-based techniques (Zhao et al., 2014), a comprehensive understanding of these compounds remains limited. In recent years, some studies have employed GC × GC to analyze vehicle-derived organics at the molecular level. For instance, Alam et al. (2018) identified a homologous series of oxygenated compounds in diesel emissions; He et al. (2022a) resolved 85% of total I/SVOCs from diesel emissions, with oxygenated I/SVOCs contributing approximately 20%; and Stewart et al. (2021) identified 94% of total non-methane organic gas (NMOG) emissions across various fuel types. Currently, emission standards in China primarily target conventional pollutants, e.g., NO_x and CO, without imposing specific limits on I/SVOCs. The effects of these emission standards upgrade on I/SVOCs remain unclear. Moreover, organics from vehicles span a wide range of

volatilities, with their composition influenced by factors such as fuel type, driving conditions, engine operations, and emission standards (Zhao et al., 2018; Tang et al., 2021). However, most existing studies focus on individual factors rather than evaluating their combined effects. Accurate characterization of vehicular I/SVOCs emissions is crucial for improving our understanding of their impacts on urban air quality and public health.

In this study, we investigated vehicular I/SVOCs at the molecular level and evaluated their contribution to SOA formation. A series of dynamometer experiments were conducted to characterize primary vehicle emissions. A fleet of in-use gasoline vehicles (GVs) (China VI) and diesel vehicles (DVs) (China IV–VI) was selected, encompassing a wide range of emission standards, mileages, and various after-treatment technologies. Non-targeted analyses were conducted using GC × GC-TOF-MS coupled with a thermal desorption system (TD). We explored the characteristics of I/SVOCs from vehicles through a comprehensive analysis of volatility distributions, chemical composition, and gas-particle partitioning at the molecular level. Furthermore, the SOA formation potential of vehicular I/SVOCs was estimated. Our study also assessed the influence of emission standards, and starting modes on I/SVOCs emissions from DVs. Additionally, we developed the organic chemical speciation profiles for vehicle emissions across the full volatility range. A molecular-level understanding of I/SVOCs chemical compositions would provide deeper insights into controlling vehicle organics emissions.

2 Materials and methods

2.1 Test vehicles, procedure, and sampling

Chassis dynamometer test was used to characterize the emissions from vehicles in both gas and particulate phases. A total of eight vehicles were tested, including four GVs and four DVs. The testing fleet consisted of DVs complying with China IV, V, and VI emission standards, as well as China VI GVs. These vehicles were selected from in-use road vehicles widely used in China, representing various model years, engine types, and aftertreatment technologies (details are provided in Table S1). All vehicles in this study underwent emission testing according to the Worldwide Harmonized Light-Duty Vehicles Test Cycle (WLTC). Each vehicle was conditioned overnight at 24 °C before testing. Two start-mode tests were conducted (cold start and one hot start), with each test condition being repeated three times. Despite the limited sample size, the experimental design and vehicle selection ensure the reliability and representativeness of the results as much as possible. Follow-up tests, such as extensive sampling of vehicles, would be beneficial for further validating our findings.

Gaseous and particulate organics from vehicle exhaust were collected following dilution using a DI-1000 system (Dekati, FI, China) (Liu et al., 2024). The systematic sampling setup is illustrated in Figs. S1 and S2. Particulate samples were directedly captured on 47 mm quartz filters (Whatman®- Sigma-Aldrich, UK) at a total flow rate of 8 L/min. Gaseous samples were collected on multiple Tenax-TA adsorbent tubes (Markes International, UK) after a polytetrafluoroethylene filter (Whatman®- Sigma-Aldrich, UK) at a flow rate of 0.6 L/min. Before sampling, the Tenax-TA tubes were conditioned with N_2 flow of 100 mL/min at 335 °C for 1 h. Before sampling, the Tenax-TA tubes were conditioned at 330 °C for 1 h, and the quartz filters were preconditioned at 550 °C for 6 h. After collection, the tubes were immediately sealed with end caps, and both filters and tubes were wrapped in aluminum foil. They were stored at −20 °C and subsequently analyzed within 10 d. Besides, Tenax-TA breakthrough experiments were conducted by connecting two tubes in series for sampling. Both the sample tube (the first one) and backup tube (the second one) were collected simultaneously, with no breakthrough observed (Fig. S3). The response in the second tube was less than 10% of that in the sample tube, indicating negligible breakthrough in the Tenax TA tubes. Field blanks of background dilution air were also collected under identical protocols for each driving cycle.

2.2 Chemical analysis and quantification of I/SVOCs

Tenax-TA tubes were analyzed using a comprehensive two-dimensional gas chromatography-mass spectrometer (EI-TOFMS 0620, Guangzhou Hexin Instrument Co., Ltd., Guangzhou, China) combined with a thermal desorption system (Markes, TD-100, UK). Quartz filters were trimmed into 10 mm round pieces and placed into pre-conditioned empty tubes before thermal desorption. The same analysis procedure was consistently applied for both the gaseous and particulate phases. The GC × GC-TOF-MS system, equipped with a solid-state modulator (SSM1810, J&X Technologies, China), was integrated into a gas chromatograph (model 7890A, Agilent Technologies, USA) and connected to a time-of-flight (TOF) mass spectrometer (EI-TOFMS 0620, Hexin, China) for

detection. The first dimension utilized a non-polar DB-5 MS column (Agilent, USA), whereas the second employed a mid-polarity DB-17 MS column (Agilent, USA) for enhanced separation. The modulation period was 6 s. The GC temperature program began at 40 °C, held steady for 5 min, ramped up at a rate of 5 °C per minute to reach 310 °C, and was subsequently held for another 5 min. The detailed parameters of TD and GC × GC-TOF-MS are provided in Tables S2 and S3. Blank samples were processed following the same methodology, and their masses were subtracted during the quantification process. The collected data were imported into Canvas (V2.5) for visualization and additional preprocessing. Typical chromatograms of samples are given in the Fig. S3.

A three-step approach was developed for the speciation and quantification of I/SVOCs. First, a set of authentic standards was introduced into pre-processed Tenax-TA tubes and analyzed using GC × GC-TOFMS, adhering to the same procedure as that used for the samples. Compounds with matching retention indices (RI) and mass spectra to the standards were easily identified. The RI corresponds to the number of carbons within an identical volatility bin along the GC column, with details provided in the supporting information. The authentic standards (1 ng/μL, Anpel, China) used in our study included 27 alkanes (3 cycloalkanes and C7–C30 n-alkanes), 7 single-ring aromatics (SRAs), 16 polycyclic aromatic hydrocarbons (PAHs), 1 aldehyde, and 1 ketone, as detailed in Table S4. The recoveries of the standards ranged from 79% to 105%. Secondly, the mass spectrums and RI database available in the NIST17 were utilized to identify the unresolved peaks. Besides, The R.Match (reverse matching factors) was used to eliminate the MS background interference and reduce the co-eluting effects of multiple species (Song et al., 2023a), thereby improving the reliability of the results. Blobs were retained if the signal-to-noise ratio > 10, R.Match > 650, and shift of RI of < 100 (Hatch et al., 2015; Song et al., 2023a). Thirdly, homologs typically display similar MS fragment patterns and peak abundance ratio, e.g., the ratio of quantifier ion to qualifier ion response. For instance, alkanes generally appear near the bottom of the chromatogram, with short retention times in the second dimension and characteristic m/z ions of 57, 85, and 71 (Song et al., 2023a). When co-elution effects are significant or contamination is present in complex samples, extracted ion chromatograms can still be used to identify key homolog features (An et al., 2020; An et al., 2021).

The calibrated quantities were determined using the standard curve and quantifier response. Calibration curves for all authentic standards were well established, with R^2 values falling between 0.95 and 0.99, indicating robust quantification (Table S4). Species without specific standards were semi-quantified using *n*-alkanes within an identical volatility bin (Zhao et al., 2014) or surrogates from similar chemical classes. A total of 438 and 424 peaks in the gas and particle phases were identified and (semi)-quantified, respectively.

2.3 Quality control and uncertainty analysis

Samples were collected by Tenax-TA tubes with a quartz filter to filter particulate matter, and breakthrough experiments were conducted prior to sampling. The actual flow rate of the pumps was calibrated both before and after each sampling session using a soap-film flowmeter. Field operational blank samples were collected daily to verify background contamination during sample storage, collection, and preparation. Duplicate samples were randomly tested, with signal intensity differences of less than 1%. After sampling, the tubes were sealed with end caps, and both the filters and tubes were wrapped in aluminum foil, stored at − 20 °C, and analyzed within 10 days.

Uncertainties associated with the analytical analysis may arise from four aspects. First, the repeatability of the analytical method. To ensure the robustness of the analytical instrument, one standard sample was analyzed for every ten samples during the GC × GC-TOF-MS analysis period. Secondly, calibration curves for all target species were carefully established to ensure the robustness of the analytical methods. Thirdly, instrument blank tests were conducted throughout the experiments, with no observable contamination detected. Lastly, uncertainties in semi-quantifying based on surrogates ranged from 21% to 57%, as detailed in the supporting information. Additionally, compounds more volatile than C7 were beyond the detection of our instruments. The breakthrough of organics with volatilities higher than C7 introduces significant uncertainties in integration and quantification. Also, capturing compounds with volatilities lower than squalene by Tenax-TA can be challenging (Song et al., 2023b). These compounds were also difficult to evaporate during thermal desorption. Additionally, compounds outside the C6–C30 range or highly oxidized organics exceeded the measurement capabilities of GC × GC.

Notably, particle-phase I/SVOCs may have been overestimated in our study. First, the organic aerosol concentration in the tailpipe was higher than in the ambient atmosphere, despite dilution within the sampling system (Zhang et al., 2024b), causing a shift in gas-particle partitioning toward the particle phase.

Additionally, the adsorption of I/SVOCs from gas phase onto filters may have introduced positive artifacts in the measured particle phase emission (Matsumoto et al., 2003). The gas/filter partition coefficient ($K_{p,face}$, m^3/cm^2) was introduced (Mader and Pankow, 2001) (details provided in the SI) to roughly quantify the overestimation caused by the adsorption of gaseous organic compounds. Our study indicates that about 1%–3% of particulate organic matter originates from the gas adsorption ($Loss_{gas}$). We highlighted adsorption as a potential source of uncertainty in our results.

2.4 Estimation of emission factors, volatility distribution, and SOA prediction

The emission factors (EFs) of I/SVOCs could be calculated based on mileage using Eq. (1) (Cao et al., 2016) and could be further converted to fuel-based EFs (Zhang et al., 2016) using fuel density and efficiency. Details are provided in the Supporting information.

$$EF_{\text{mileage-based}} = \frac{1000VD_rC_iM_i}{RL}, \quad (1)$$

where EF represents the emission factors (mg/km); V denotes the sampling volume (L) within standard condition (273.12 K, 101.33 kPa); Dr represents the rate of dilution; and C_i refers to the concentration of species i; M_i indicates the relative molecular mass of species i; and R represents the molar volume of species i at standard condition (273.12 K, 101.33 kPa), which is 22.4 L/mol; L refers to the test route length (km).

The volatility distribution of the identified organics was determined based on effective saturation concentration (C^*, μg/m^3) (Lu et al., 2018; Huo et al., 2021b). Each volatility bin of 10^n μg/m^3 spans a range in logarithmic space from $C^* = 0.3 \times 10^n$ to $C^* = 3 \times 10^n$, where n varies from − 1 to 8. The classification includes VOCs ($C^* > 3 \times 10^6$), IVOCs ($300 < C^* < 3 \times 10^6$) and SVOCs ($0.3 < C^* < 300$). The C* values were calculated using the following equation (Eq. (2)) (Donahue et al., 2012; Lu et al., 2018; Huo et al., 2021b):

$$C_i^* = \frac{M_i 10^6 \xi_i P_{L,i}^0}{760RT}, \quad (2)$$

where M_i represents the molecular weight of compound i (g/mol), and ξ_i denotes the activity coefficient of species i within the condensed phase, with an assumed value of 1. $P_{L,i}^0$ denotes the subcooled liquid saturation vapor pressure of pure species i at 298 K, based on data from the EPI Suite (Estimation Programs Interface) developed by the US EPA, available from the U.S. Environmental Protection Agency (EPA) website.

The calculation of SOA formation potential was based on the equation (Eq. (3)):

$$SOA_p = \sum EF_i \times \left(1 - e^{-K_{\text{OH},i} \times [\text{OH}] \times \Delta t}\right) \times Y_i, \quad (3)$$

where EF_i represents the EF of a species i, $k_{\text{OH},i}$ denotes the reaction rate constant of compound i with OH (cm^3/(molec·s)); and [OH] indicates the OH concentration (molec/cm^3). The SOA yield (Y_i) values were obtained from the literature (Chan et al., 2009; Chan et al., 2010; Loza et al., 2014; Harvey and Petrucci, 2015; Algrim and Ziemann, 2016; Li et al., 2016; Liu et al., 2018; Mcdonald et al., 2018; Algrim and Ziemann, 2019). The SOA yields utilized in our study correspond to high-NO_x conditions, considering the high-NO_x environment associated with vehicle emissions. $[\text{OH}] \times \Delta t$ represents the OH exposure, defined as 14.4×10^{10} (molec·s)/cm^3 (roughly corresponding to 1.1 d at an OH concentration of 1.5×10^6 molec/cm^3) (Song et al., 2022). This calculation involves estimating the SOA formation potential for each VOC and I/SVOCs species, incorporating a more precise volatility distribution, a wider range of speciated compounds, SOA yields, and OH reaction rate. The values are provided in Table. D1 of the supporting data. Notably, we acknowledge that the method represents a zeroth-order approximation for comparing SOA formation potentials. Multi-generation oxidation chemistry and aerosol aging are likely to play an as-yet undetermined role beyond the timescale over which these SOA yields were measured (Chan et al., 2009).

We also quantified the SOA formation potential based on the bin method. In this approach, species were categorized into different bins based on the retention times of n-alkanes according to Zhao et al. (2015; 2016). In brief, the total ion chromatogram of I/SVOCs was divided into 24 bins, with each bin corresponding to the retention time of a specific n-alkane. The beginning and ending times for each bin were defined based on the average retention times of two neighboring n-alkanes. As an example, the starting time for bin 14 (B14) was defined by the mean retention time of C13 and C14, whereas the ending time for B14 was calculated as the mean retention time of C14 and C15. Details are given in supporting information. The SOA formation potential was also calculated utilizing the SOA yield and OH reactivity of a certain n-alkane to represent all the species in the same bin grouped with retention time (Zhao et al., 2015; 2016). For example, the species in the B14, the SOA yield, and the OH reactivity of C14 were used to represent all the species in the B14 group (Table S5 and Support data).

3 Results and discussion

3.1 Primary emissions of I/SVOCSs from vehicle exhausts

The EFs for total organic compounds from China VI GVs and DVs in both gas and particle phases are presented in Fig. 1. Overall, the EFs for DVs under China IV to China VI emission standards ranged from 21.3 to 3241.8 mg/(kg·fuel). It was slightly higher than those reported by Alam et al. (27–160 mg/kg·fuel), likely due to differences in testing conditions. Alam et al. (2019) focused on steady-state light diesel engines, whereas our study employed a unified driving cycle (WLTC) that encompassed various driving modes, e.g., acceleration and deceleration, which tend to increase I/SVOCs emissions. In contrast, our results were lower than those of He et al. (2022b) (1.7–18900 mg/(kg·fuel)), likely due to the inclusion of older China IV heavy diesel trucks with longer service lifetimes in their study. The EFs for GVs (114.4 ± 42.1 mg/(kg·fuel)) were notably lower than those for DVs in both the gaseous and particulate phases. Diesel fuels contain more complex hydrocarbons than gasoline fuels (Jathar et al., 2014), which contribute to increased I/SVOCs production during incomplete combustion. Additionally, the compression ignition mechanism and lower exhaust temperatures in diesel engines hinder the complete decomposition or removal of these compounds (Gentner et al., 2017), resulting in significantly higher emissions compared to GVs.

The EFs of total organics in the particle phase were slightly higher than those in gas phase, accounting for 51.3% ± 10.4% and 65.5% ± 7.8% of total organics for GVs and DVs, respectively. In the gas phase, VOCs dominated the measured organic emissions, accounting for 70.4% and 51.7% for GVs and DVs, respectively. In particle phase, they accounted for only 3.7% and 3.5%, respectively (Fig. 1 and S4). Conversely, I/SVOCs were the primary components in the particle phase, comprising 93.7% and 94.9% of emissions from GVs and DVs, respectively. This composition was similar to emissions from incense-burning smoke (85.9%) (Song et al., 2023b) and higher than those observed from ships (~60%) (Huang et al., 2018), biomass combustion (82%–91%), and cooking emissions (81.4%) (Huo et al., 2021a). It should be noted that the limited detection capability of GC × GC-MS resulted in incomplete coverage of VOC species, likely leading to an overestimation of the I/SVOC proportion. To quantify the underestimation of VOCs, we incorporated VOCs data of GVs analyzed by GC-MS from our

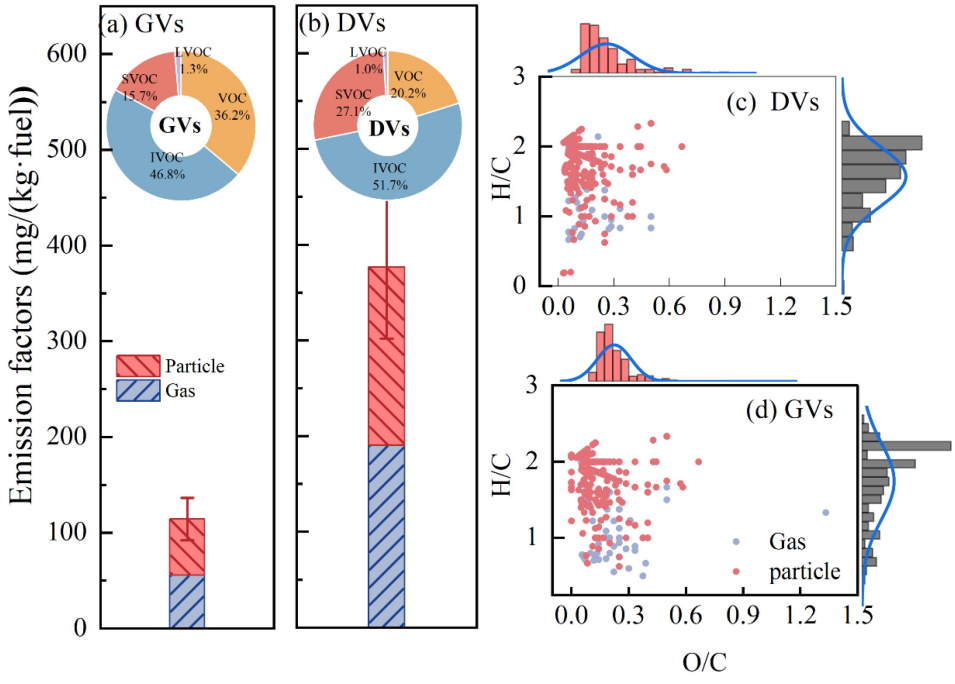

Fig. 1 Emission factors of I/SVOCs from China VI vehicles in both gas and particle phase: (a) gasoline vehicles (GVs) and (b) diesel vehicles (DVs); the pie chart displays the volatility distributions based on C^*; the error bar represents uncertainty range of the total EFs; the Van-Krevelen diagrams and the frequency histogram of O/C and H/C for China VI (c) DVs and (d) GVs.

published study (Liu et al., 2024). The good comparability (± 21.3%) of these overlapping species from GCMS and GC × GC-MS (e.g., undecane, 1,4-Methylethylbenzene) demonstrates that data merging was feasible. The results showed that using GC × GC-TOFMS exclusively for vehicle exhaust testing could underestimate VOCs by about 36% (Fig. S5), leading to an overestimation of the I/SVOC proportion in turn. The underestimation applies only to vehicle exhaust emissions. It is important to emphasize that the analysis of our study was based on GC × GC-MS. Although the limitation may affect the relative proportions of VOCs and I/SVOCs, it does not alter the overall conclusions and the scientific significance.

Van-Krevelen diagrams were utilized to characterize the chemical structure of organic species by plotting the ratio of H/C against the O/C ratio (Laszakovits and Mackay, 2022). In our study, the molecular composition of I/SVOCs from both vehicle types was similar, with the majority of species concentrated in the region where the H/C ratio exceeded 0.5 and the O/C ratio was below 0.6. The distribution of I/SVOCs from DVs was more dispersed, particularly in the particle phase, suggesting a higher oxidation state compared to emissions from GVs. The double bond equivalent (DBE) value offers insight into the unsaturation of a compound (Huo et al., 2021a). By combining the Van-Krevelen diagram with DBE, differences in the molecular structures across various emissions were further emphasized. As shown in Fig. 2, the size denotes EFs, while the color represents the ratio of oxygen and carbon (O/C). In the gas phase, I/SVOCs from DVs were concentrated in the low DBE range (0–3), while those from GVs were found in the middle and high DBE ranges (Figs. 2(a) and 2(b)). This difference likely reflects the higher proportion of aromatics in gasoline fuel, which typically exhibits more compact structures, lower H/C ratios, and higher DBE values (Chacon-Madrid and Donahue, 2011). The most unsaturated compounds in diesel emissions were phenyl-substituted ketones, whereas polycyclic aromatic hydrocarbons (e.g., benzopyrene) dominated gasoline emissions. Besides, in the particle phase, the organics exhibit a high oxidation state and significant dispersion, particularly those from DVs. These findings could offer a deeper understanding of the molecular composition and chemical structure characteristics of different vehicle emissions and offer an important basis

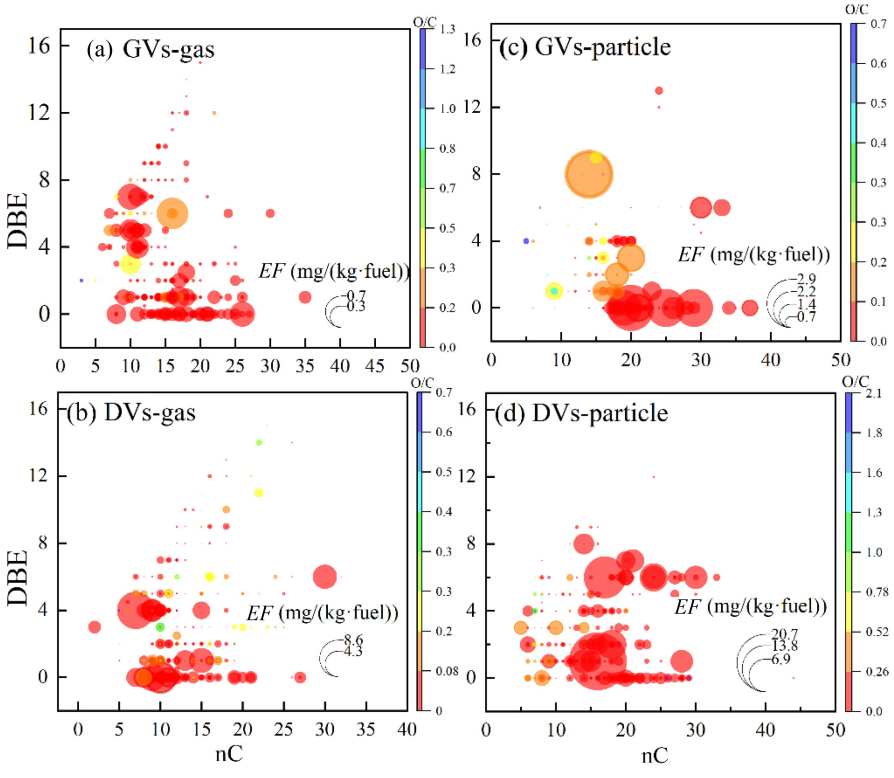

Fig. 2 The DBE versus carbon number maps of I/SVOCs emitted from China VI diesel and GVs in both gas and particle phases. The color mapping indicates the O/C ratio of I/SVOCs, and the bubble size indicates the emission factors of I/SVOCs. The gas emission from (a) GVs and (b) DVs; the particle emission from (c) GVs and (d) DVs.

for assessing their environmental impact.

3.2 Chemical composition, gas-particle partitioning, and volatility distributions of measured I/SVOCs

The volatility of organic compounds largely determines their phase in the atmosphere, thereby influencing their oxidation efficiency and contribution to pollutant formation (Donahue et al., 2012; Lu et al., 2018). The volatile distributions of organics are crucial for understanding their distribution mechanisms between gas and particle phases. Figures 3(a) and 3(b) illustrate the volatility distributions in the particulate and gaseous phases for DVs and GVs. Overall, DVs exhibited higher particulate emissions, while GVs showed elevated gas-phase emissions. In DVs, I/SVOCs ($Log_{10}C^*$ = 2–6) dominated the total emission, especially in particulate phase. VOCs were primarily found in the gas phase, while SVOCs contributed more to the particulate phase. In contrast, GVs exhibited more pronounced gaseous emissions, particularly in the $log_{10}C^*$ range of 7–8. Based on their carbon skeleton, organic compounds can be categorized as aliphatic, alicyclic, aromatic, and heterocyclic and further classified according to functional groups. The distribution of various organics between gas and particle phases is shown in Figs. S6 and 3. Alkanes exhibited a similar proportion in gas and particle phases, indicating a uniform distribution across the volatility range. Aromatics, including the SRAs and PAHs, were predominantly found in the gas phase, accounting for over 88.2% of emissions from GVs. Diesel vehicle emissions contain a higher proportion of SRAs in the particulate phase (75.4%), attributed to lower combustion temperatures and an inherently higher proportion of SRAs in fuel (Jathar et al., 2014). Additionally, both gasoline and diesel emissions show a tendency for oxygenated I/SVOCs, such as n-alkanoic acids, furfural, and aldehydes, to partition into the particle phase due to their lower volatility, resulting in a significantly higher particle-phase distribution compared to the gas phase (Zhang et al., 2024b). It is essential to recognize that the gas-particle partitioning observed in this study may overestimate the particle-phase emissions. Particle-phase emissions were collected on quartz filters, which can adsorb gas-phase I/SVOCs, leading to positive sampling artifacts in particle-phase measurements (Zhang et al., 2024b). Furthermore, in our study, the gas-particle partitioning reflects only the I/SVOC distribution within vehicle exhausts, rather than in the atmosphere, where lower temperatures and varying particle substrates alter the distribution (Alam et al., 2019).

As shown in Figs. 3(c)–3(e) and Fig. 4, gaseous emissions from gasoline and DVs primarily consist of aliphatic compounds and aromatics, predominantly distributed within the high volatility range ($Log_{10}C^*$ = 6–8). The dominant compound groups of I/SVCOs emitted by vehicles were alkanes (including n/b-alkanes, 29.7%–41.9%), single-ring aromatics (2.6%–

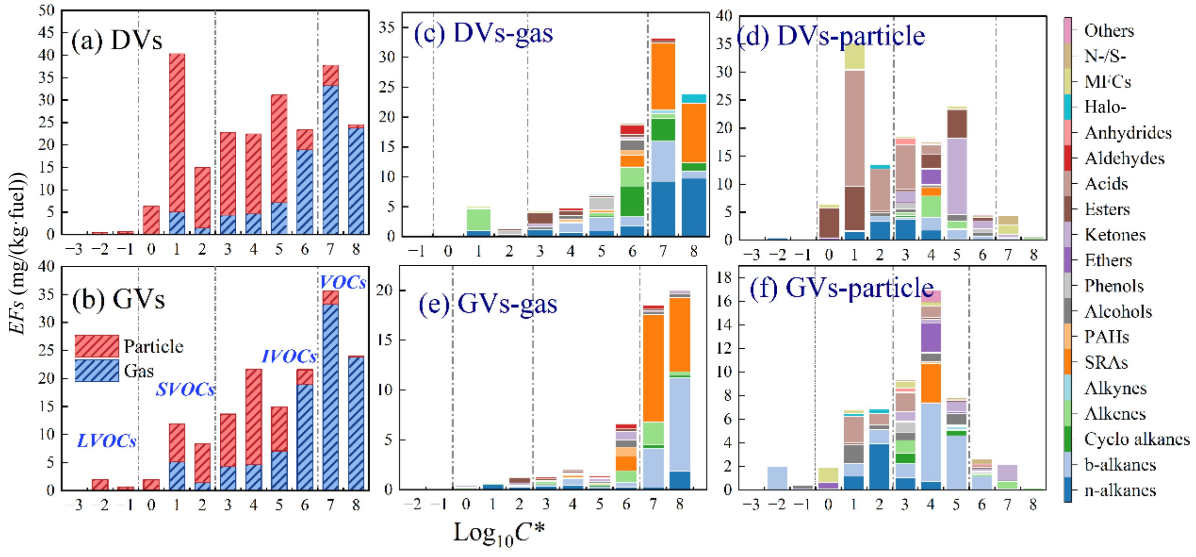

Fig. 3 The volatility distribution of organics in gas and particulate phases from China VI vehicles. (a) and (b) were the emission of DVs and GVs in both gas and particulate phase; (c) and (d) were the gas and particulate phase of DVs; (e) and (f) were the gas and particulate phase of GVs (SRAs: Single-ring aromatics; MFCs: Multi-functional Compounds; Halo-: Haloalkanes). The data are provided in Table D2 of the supporting data.

29.8%), and cycloalkanes (1.0%–13.1%), consistent with previously reported results (Zhang et al., 2024b). The SRAs were mainly present in the gas phase, accounting for 28.0% and 18.5% of gasoline and DVs, respectively, largely due to incomplete fuel combustion. Notably, most SRAs fall within the VOC range accounting for 17.0% and 26.7% of gas-phase emissions from GVs and DVs; while in the I/SVOCs range, SRAs only account for 2.1% and 3.1% of total gasoline and DVs emission, respectively. These compounds mainly comprise high-carbon alkylbenzenes with variations in chain length, ring structures, and branched alkyl substituents, aligning with findings by (Drozd et al., 2019). Additionally, cycloalkanes in DVs were significantly higher than in GVs, particularly in the gas phase, accounting for 13.5% of total emissions compared to 3.5% in GVs. In DVs, the diversity of straight-chain, branched-chain, and cyclic hydrocarbons in diesel fuel contributes to the high presence of aliphatic and cyclic compounds (> 65%) (Jathar et al., 2014; Alam et al., 2018). In contrast, gasoline, which has higher aromatic content, leads to elevated emissions of aromatic compounds in its gas-phase exhaust. Compared to gaseous emissions, aliphatic compounds made up a larger fraction of the particle phase, comprising 73.2% and 70.4% in DVs and GVs; Alkanes remain the dominant group, similar to their prevalence in gas-phase emissions (Fig. 4). However, cycloalkanes, which were prevalent in gas phase, exhibited a noticeable decrease in particle phase. Oxygenated I/SVOCs (O–I/ SVOCs, e.g., acids, esters and ketones) has a more significant proportion in

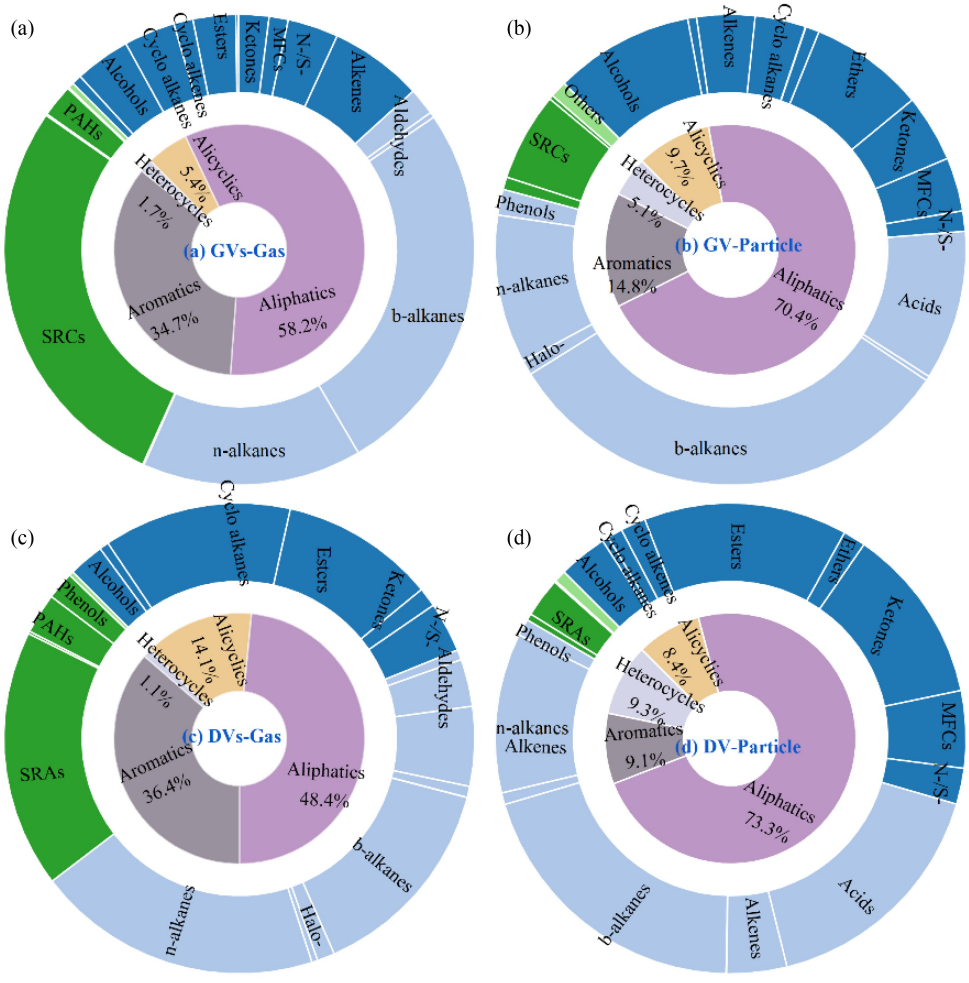

Fig. 4 The Sunburst diagrams for the classifications and their contribution of identified chemical species from vehicles. The compounds are categorized in the inner and outer circles according to their carbon backbone and functional group information: (a) gasoline vehicle gas phase; (b) gasoline vehicle particulate phase; (c) diesel vehicle gas phase; (d) diesel vehicle particulate phase (SRAs: Single-ring aromatics; MFCs: Multi-functional Compounds). The data are provided in Table. D3 of the supporting data.

particulate phases (40.3%–56.8%) compared with gas phases (14.4%–15.3%) in gasoline and DVs in our study. Alam et al. (2019) reported that oxygen-containing compounds appear exclusively in the particle phase of diesel engine emissions, constituting up to 37%. The formation of these compounds in the engine primarily results from oxidation during combustion; for instance, aldehydes and ketones can be produced by hydrogen abstraction with peroxyalkyl radicals (Wagner and Wyszyński, 1996). O-I/SVOCs in the gas phase, generated during the combustion process in the engine, are often challenging to identify using traditional GC-MS. Our study successfully identified and quantified these O-I/SVOCs species using the high-resolution instrument and could offer new insights into vehicle emissions. Understanding these distribution characteristics is crucial for developing more effective vehicle emission control strategies and mitigating air pollution.

3.3 Influences of emission standards, and starting mode on the I/SVOCs emission

Figure 5(a) compares the composition of I/SVOCs emissions from China VI DVs under various operating conditions. As expected, the advancement of emission standards significantly reduced emission levels of various organic compounds from DVs, although reduction efficiencies varied among different compounds. The average organic EFs of DVs decreased markedly, from 3504.3 mg/(kg·fuel) under China IV standards to 376.7 mg/(kg·fuel) under China VI standards, representing a reduction of 89.2%. Similarly, previous studies (Drozd et al., 2019) have found that emissions reduced by nearly an order of magnitude from vehicles with minimal controls (T0) to those with the most advanced technologies. This reduction was primarily due to enhanced combustion efficiency and the integration of after-treatment technologies in modern vehicles, which reduce incomplete fuel combustion and enhance catalytic performance (Huang et al., 2015). Notably, the reduction in EFs of organics from China IV to China V vehicles (77.6%) was slightly higher than from China V to VI vehicles (52.2%). In our study, we primarily focus on the emissions from in-use vehicles, as those with lower emission standards typically have longer service lives and higher mileage on roadways. As mileage increases, the emission control systems, e.g., the catalytic converters and particulate filters, gradually deteriorate or fail, resulting in elevated emissions. Considering that our tested vehicles are in-use vehicles, these differences across different emission standards reflects the combined effects of emission standard upgrades and vehicle aging caused by the use of vehicles. This emphasizes the importance of phasing out older vehicles or upgrading emissions control technologies to more effectively reduce I/SVOCs emissions.

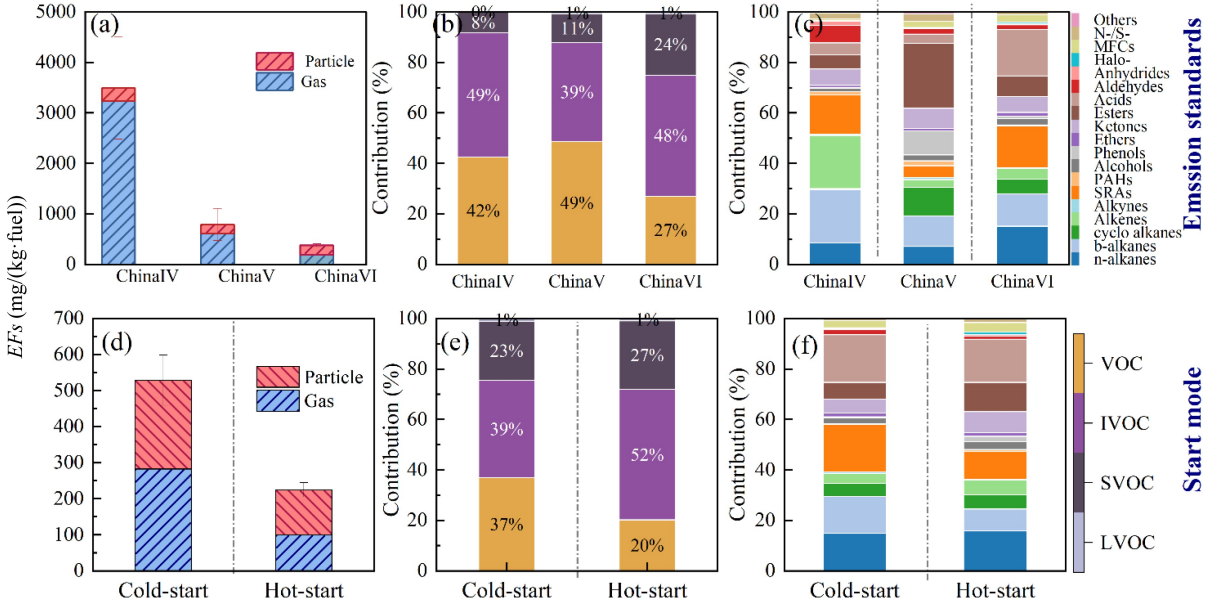

Fig. 5 The (a) *EFs*, (b) volatility distribution and (c) composition of I/SVOCs from DVs with various emission standards; and (d) *EFs*, (e) volatility distribution and (f) composition of I/SVOCs under different starting mode with China VI-DVs. The data are provided in Table D4 of the supporting data.

Regarding classified organics across different volatility ranges, the EFs of VOCs showed the most significant decrease under stricter emission standards. Compared to China IV vehicles, the EFs of VOC for China V and VI vehicles were reduced by 71.5% and 94.5%, respectively. In contrast, control of I/SVOCSs was less pronounced, a trend also observed in gasoline vehicle emissions (Qi et al., 2021). While the absolute EFs of I/SVOCs declined from China IV to China VI-DVs significantly, their relative mass fraction increased. For instance, the proportion of I/SVOCs rose substantially with upgraded standards, particularly for SVOCs, which increased from 8.2% ± 1.4% in China IV vehicles to 11.3% ± 2.3% and 24.4% ± 2.3% in China V and VI vehicles, respectively (Fig. 5(b)). Additionally, alkanes and PAHs gradually decreased with stricter standards, while the decrease in oxygenated I/SVOCs (e.g., alcohols, phenols, and aldehydes) was not significant, and their relative proportions even increased noticeably (Figs. S7 and 5(c)). These findings suggest that while the control measures were effective in reducing total organic emissions, they did not uniformly remove all substances, and may have led to a relative increase in certain oxidized compounds. Our results highlight that future emission control technologies for DVs should prioritize further reduction of I/SVOCs emissions while maintaining effective VOC control (Zhang et al., 2023).

The total EFs for cold-start were higher (528.4 mg/(kg·fuel)) compared to those for hot-start (224.8 mg/(kg·fuel)), reflecting reduced catalytic converter efficiency during cold-start. During cold-start conditions, low engine temperatures lead to incomplete combustion and suboptimal performance of the exhaust after-treatment system, which has not yet reached its optimal operating temperature for effective pollutant removal. Previous studies have also indicated that cold-start operation results in higher total hydrocarbon emissions compared to hot-start (Drozd et al., 2016; Zhao et al., 2018). Although the EFs from cold-start conditions were significantly higher than those from hot-start conditions, the relative proportions of each component showed different trends (Fig. 5(d)). As illustrated in Figs. S8 and 5(e), the total proportion of I/SVOCs was higher in hot-start conditions (78.8%) compared to cold-start conditions (62.0%). This difference is likely due to elevated engine and exhaust temperatures in hot-start conditions, which improve combustion efficiency and facilitate more complete volatilization and combustion of unburned fuel and lubricating oil (Alam et al., 2018). Additionally, the emission composition varied between cold and hot starts. During cold starts, alkanes and PAHs were more prevalent, while oxidation products (e.g., acids and esters) were relatively less abundant (Figs. S8 and 5(f)). Esters (11.6%), ketones (8.3%) and alcohols (3.2%) were notably more abundant under cold-start conditions. This suggests that incomplete combustion and lower exhaust temperatures during cold starts would inhibit the oxidation of organic compounds (Zhao et al., 2018; Zhang et al., 2024b). In contrast, the elevated temperatures during hot starts promote more complete combustion and oxidation.

3.4 Impacts of speciated I/SVOCs on SOA prediction

The potential for SOA formation from gas-phase I/SVOCs based on the hot-start emission of China VI vehicles was estimated. The contributions of various groups to the SOA formation potential are illustrated in Fig. 6. Notably, I/SVOCs were the primary contributors to SOA formation, indicating a significantly higher SOA yield efficiency compared to VOCs. Specifically, I/SVOCs accounted for 82.2% and 69.9% of SOA production in diesel and GVs, respectively. In contrast, they made up only 50.9% and 42.7% of the EFs in DVs and GVs (Figs. 6 and S4). The significant contribution of I/SVOCs to SOA formation could be attributed to their higher yields and reaction rates with OH radicals, as demonstrated in various emissions studies, including cooking emissions (Song et al., 2022), gasoline exhaust (Zhao et al., 2014; Du et al., 2018; Qi et al., 2021; Huang et al., 2024), and coal combustion (Hatch et al., 2015; Huo et al., 2021b).

Alkanes played a significant role in the predicted SOA formation potential for both DVs and GVs, contributing 28.1% and 38.3%, respectively, followed by alkenes. C14–C18 alkanes were the primary contributors in GVs, whereas alkanes larger than C21 dominated in DVs, largely due to differences in fuel composition. Among alkenes, squalene was identified as the major contributor to SOA formation potential in DVs. O-I/SVOCs also made significant contributions to SOA formation potential for both GVs and DVs, with esters (12.1% and 10.9% for DVs and GVs), phenols (9.7% and 10.6% for DVs and GVs), and ketones (1.2% and 9.4% for DVs and GVs) showing high potential. These differences reflect variations in vehicle and fuel characteristics. Compared to unoxidized I/SVOCs, the higher oxidation state and polarity of O-I/SVOCs enhance their potential to participate in SOA formation (Huang et al., 2024). This finding underscores the pivotal role of O-I/SVOCs in SOA formation, emphasizing their importance in future fine particulate control strategies.

We further compared the SOA formation potential

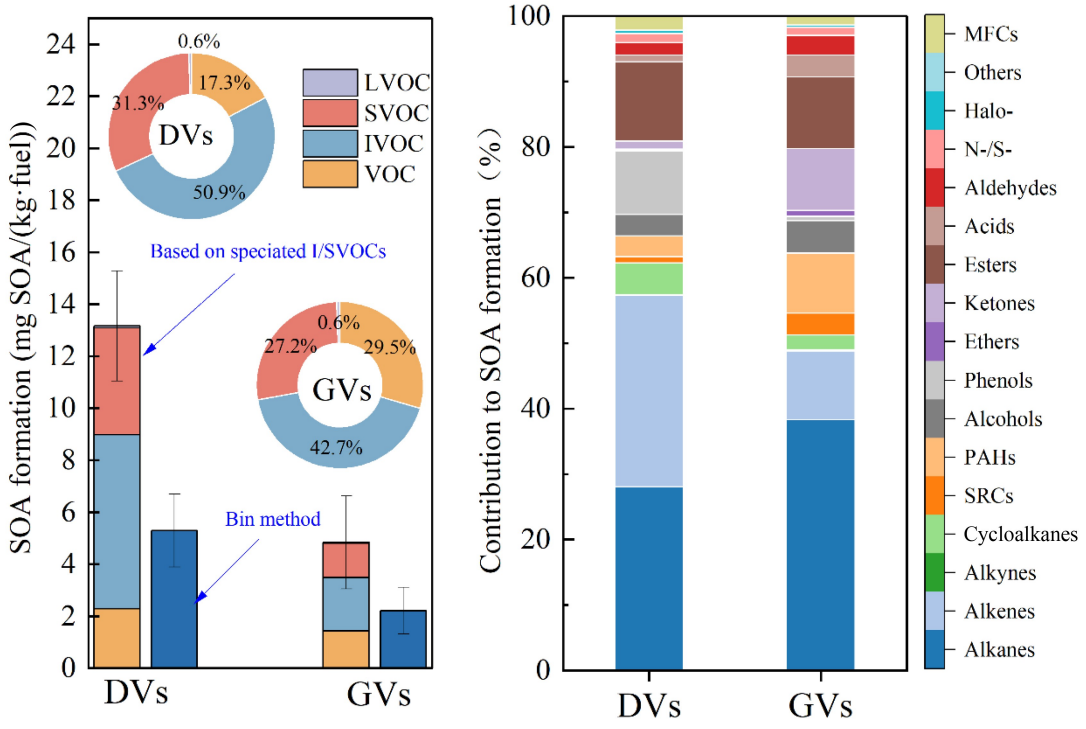

Fig. 6 The SOA formation estimation for DVs and GVs in the gas phase.

calculated using two different parametric approaches, i.e., the bin method and the speciated compounds method. The former is a commonly adopted method that utilizes the SOA yield and OH reactivity of a certain n-alkane to represent all species in the same bin (Zhao et al., 2015, 2016). The latter involves estimating the SOA formation potential for each VOC and I/SVOCs species, incorporating a more precise volatility distribution, a wider range of speciated compounds, SOA yields, and OH reaction rate. As illustrated in Fig. 6, the speciated compounds method significantly increased SOA production estimates by 1.5 times for DVs and 1.2 times for GVs, respectively.

Previous laboratory studies have found that the substantial SOA formation potential measured from vehicle exhaust cannot be fully explained by the SOA yield of VOCs (Peng et al., 2017; Du et al., 2018; Zhang et al., 2023), even when some I/SVOCs precursors are included (Zhang et al., 2024a). Our results suggest that reducing the proportion of UCMs through appropriate techniques could partially address the underestimation of SOA production. Enhancing control of I/SVOCs would be more effective in mitigating fine particle pollution.

4 Conclusions and implications

Vehicular emissions are significant anthropogenic sources of I/SVOCs in urban cities. Neglecting these compounds may lead to a substantial underestimation of SOA formation. In this study, we applied a non-targeted analysis approach using comprehensive two-dimensional gas chromatography coupled with mass spectrometry (GC × GC-TOF-MS) to chemically characterize I/SVOCs of exhaust emissions from DVs and GVs. The vehicles tested covered a range of emission standards and were equipped with various after-treatment devices. A comprehensive molecular-level characterization of I/SVOCs in vehicular emissions, including their chemical composition, volatility distributions, and gas-particle partitioning were obtained. Furthermore, the SOA formation potential of vehicle exhausts based on speciated I/SVOCs was estimated and compared to that using unspeciated compounds. The comparison enabled an evaluation of the accuracy of SOA potential estimates. These findings can contribute to improving the I/SVOCs emission inventory in China and enhance further simulations of SOA formation.

The high-resolution GC × GC-TOFMS technology, through speciation testing, facilitates a more comprehensive identification and quantitative analysis of various I/SVOCs in exhaust emissions. In our study, over 400 species were identified and categorized by

their properties, exhibiting a wide range of volatilities. Emissions from DVs contribute more to I/SVOCs than those from GVs. Gas-phase emissions are primarily concentrated in the VOC volatility range, while particle-phase emissions are predominantly found in the I/SVOCs volatility range. Aliphatic alkanes are the major components of I/SVOC emissions from China VI vehicles, with particle-phase emissions showing minimal variation across fuel types and a higher concentration of O-I/SVOCs. Notably, stricter emission standards for DVs significantly reduce organic emissions, particularly gaseous compounds, demonstrating the effectiveness of advanced control technologies. However, control over I/SVOCs is less effective, resulting in a higher proportion of oxidized products. Additionally, the detailed chemical composition provided by speciation testing greatly improved the accuracy of SOA generation potential estimates by more than 100% compared to traditional unspeciated species methods. Our findings highlight the critical role of I/SVOCs from diesel and GVs in air pollution and provide a scientific basis for more effective vehicle emission control and air quality management strategies.

While our finding offers valuable insights into the emission factors and SOA formation potential of I/SVOCs from vehicles, several limitations should be considered. We emphasize that the limited number of vehicles in our study may lead to incidental results. Despite the limited sample size, the experimental design and vehicle selection ensure the reliability and representativeness of the results as much as possible. Follow-up tests, such as extensive sampling of vehicles, would be beneficial for further validating our findings. On the other hand, the gas-particle partitioning observed in this study may overestimate particle-phase emissions. Particle-phase emissions were collected on quartz filters, which can adsorb gas-phase I/SVOCs, leading to positive sampling artifacts in the measurement of particle-phase emissions. The gas-particle partitioning reported here reflects only the distribution of I/SVOCs within vehicle exhausts, rather than in the atmosphere, where lower temperatures and varying particle substrates may alter the distribution. Furthermore, it is important to note that each of the analytical techniques used in this study has its limitations. For example, GC × GC analysis lacks real-time information, and PTR-ToF-MS analysis can not differentiate between isomers of gaseous organics. Therefore, combining multiple online and offline measurement techniques in future studies could help mitigate these limitations, as they would provide complementary data to address the shortcomings of individual methods.

Conflict of Interests Jianfei Peng is a youth editorial board member of Frontiers of Environmental Science & Engineering. And the authors declare that the research was conducted in the absence of any commercial or financial relationships that could be construed as a potential conflict of interest.

Acknowledgements This work was financially supported by the National Key Research and Development Program of China (Nos. 2023YFC3706201 and 2022YFE0135000), the National Natural Science Foundation of China (Nos. 42175123 and 42311530112), and the Fundamental Research Funds for the Central Universities of China (Nos. 63241318, 63241322, and 63243126).

Electronic Supplementary Material Supplementary material is available in the online version of this article at https://doi.org/10.1007/s11783-025-1990-y and is accessible for authorized users.

References

Alam M S, Zeraati-Rezaei S, Liang Z, Stark C, Xu H, MacKenzie A R, Harrison R M (2018). Mapping and quantifying isomer sets of hydrocarbons (≥C12) in diesel exhaust, lubricating oil and diesel fuel samples using GC×GC-ToF-MS. Atmospheric Measurement Techniques, 11(5): 3047–3058

Alam M S, Zeraati-Rezaei S, Xu H, Harrison R M (2019). Characterization of gas and particulate phase organic emissions (C9–C37) from a diesel engine and the effect of abatement devices. Environmental Science & Technology, 53(19): 11345–11352

Algrim L B, Ziemann P J (2016). Effect of the keto group on yields and composition of organic aerosol formed from OH radical-initiated reactions of ketones in the presence of NO_x. Journal of Physical Chemistry A, 120(35): 6978–6989

Algrim L B, Ziemann P J (2019). Effect of the hydroxyl group on yields and composition of organic aerosol formed from OH radical-initiated reactions of alcohols in the presence of NO_x. ACS Earth & Space Chemistry, 3(3): 413–423

An Z, Li X, Shi Z, Williams B J, Harrison R M, Jiang J (2021). Frontier review on comprehensive two-dimensional gas chromatography for measuring organic aerosol. Journal of Hazardous Materials Letters, 2: 100013

An Z, Ren H, Xue M, Guan X, Jiang J (2020). Comprehensive two-dimensional gas chromatography mass spectrometry with a solid-state thermal modulator for *in-situ* speciated measurement of organic aerosols. Journal of Chromatography. A, 1625: 461336

Cao X, Yao Z, Shen X, Ye Y, Jiang X (2016). On-road emission characteristics of VOCs from light-duty gasoline vehicles in Beijing, China. Atmospheric Environment, 124: 146–155

Chacon-Madrid H J, Donahue N M (2011). Fragmentation vs. functionalization: chemical aging and organic aerosol formation. Atmospheric Chemistry and Physics, 11(20): 10553–10563

Chan A W H, Chan M N, Surratt J D, Chhabra P S, Loza C L,

Crounse J D, Yee L D, Flagan R C, Wennberg P O, Seinfeld J H (2010). Role of aldehyde chemistry and NO_x concentrations in secondary organic aerosol formation. Atmospheric Chemistry and Physics, 10(15): 7169–7188

Chan A W H, Kautzman K E, Chhabra P S, Surratt J D, Chan M N, Crounse J D, Kürten A, Wennberg P O, Flagan R C, Seinfeld J H (2009). Secondary organic aerosol formation from photooxidation of naphthalene and alkylnaphthalenes: implications for oxidation of intermediate volatility organic compounds (IVOCs). Atmospheric Chemistry and Physics, 9(9): 3049–3060

Dallüge J, Beens J, Brinkman U A T (2003). Comprehensive two-dimensional gas chromatography: a powerful and versatile analytical tool. Journal of Chromatography. A, 1000(1−2): 69–108

Donahue N M, Kroll J H, Pandis S N, Robinson A L (2012). A two-dimensional volatility basis set – Part 2: Diagnostics of organic-aerosol evolution. Atmospheric Chemistry and Physics, 12(2): 615–634

Drozd G T, Zhao Y, Saliba G, Frodin B, Maddox C, Oliver Chang M C, Maldonado H, Sardar S, Weber R J, Robinson A L, et al. (2019). Detailed speciation of intermediate volatility and semi-volatile organic compound emissions from gasoline vehicles: effects of cold-starts and implications for secondary organic aerosol Formation. Environmental Science & Technology, 53(3): 1706–1714

Drozd G T, Zhao Y, Saliba G, Frodin B, Maddox C, Weber R J, Chang M C O, Maldonado H, Sardar S, Robinson A L, et al. (2016). Time resolved measurements of speciated tailpipe emissions from motor vehicles: trends with emission control technology, cold start effects, and speciation. Environmental Science & Technology, 50(24): 13592–13599

Du Z, Hu M, Peng J, Zhang W, Zheng J, Gu F, Qin Y, Yang Y, Li M, Wu Y, et al. (2018). Comparison of primary aerosol emission and secondary aerosol formation from gasoline direct injection and port fuel injection vehicles. Atmospheric Chemistry and Physics, 18(12): 9011–9023

Gentner D R, Jathar S H, Gordon T D, Bahreini R, Day D A, El Haddad I, Hayes P L, Pieber S M, Platt S M, De Gouw J, et al. (2017). Review of urban secondary organic aerosol formation from gasoline and diesel motor vehicle emissions. Environmental Science & Technology, 51(3): 1074–1093

Harvey R M, Petrucci G A (2015). Control of ozonolysis kinetics and aerosol yield by nuances in the molecular structure of volatile organic compounds. Atmospheric Environment, 122: 188–195

Hatch L E, Luo W, Pankow J F, Yokelson R J, Stockwell C E, Barsanti K C (2015). Identification and quantification of gaseous organic compounds emitted from biomass burning using two-dimensional gas chromatography–time-of-flight mass spectrometry. Atmospheric Chemistry and Physics, 15(4): 1865–1899

He X, Zheng X, You Y, Zhang S, Zhao B, Wang X, Huang G, Chen T, Cao Y, He L, et al. (2022a). Comprehensive chemical characterization of gaseous I/SVOC emissions from heavy-duty diesel vehicles using two-dimensional gas chromatography time-of-flight mass spectrometry. Environmental Pollution, 305: 119284

He X, Zheng X, Zhang S, Wang X, Chen T, Zhang X, Huang G, Cao Y, He L, Cao X, et al. (2022b). Comprehensive characterization of particulate intermediate-volatility and semi-volatile organic compounds (I/SVOCs) from heavy-duty diesel vehicles using two-dimensional gas chromatography time-of-flight mass spectrometry. Atmospheric Chemistry and Physics, 22(21): 13935–13947

Huang C, Hu Q, Li Y, Tian J, Ma Y, Zhao Y, Feng J, An J, Qiao L, Wang H, et al. (2018). Intermediate volatility organic compound emissions from a large cargo vessel operated under real-world conditions. Environmental Science & Technology, 52(21): 12934–12942

Huang D D, Hu Q, He X, Huang R J, Ding X, Ma Y, Feng X, Jing S A, Li Y, Lu J, et al. (2024). Obscured contribution of oxygenated Intermediate-volatility organic compounds to secondary organic aerosol formation from gasoline vehicle emissions. Environmental Science & Technology, 58(24): 10652–10663

Huang L, Bohac S V, Chernyak S M, Batterman S A (2015). Effects of fuels, engine load and exhaust after-treatment on diesel engine SVOC emissions and development of SVOC profiles for receptor modeling. Atmospheric Environment, 102: 228–238

Huo Y, Guo Z, Li Q, Wu D, Ding X, Liu A, Huang D, Qiu G, Wu M, Zhao Z, et al. (2021a). Chemical fingerprinting of HULIS in particulate matters emitted from residential coal and biomass combustion. Environmental Science & Technology, 55(6): 3593–3603

Huo Y, Guo Z, Liu Y, Wu D, Ding X, Zhao Z, Wu M, Wang L, Feng Y, Chen Y, et al. (2021b). Addressing unresolved complex mixture of I/SVOCs emitted from incomplete combustion of solid fuels by nontarget analysis. Journal of Geophysical Research: Atmospheres, 126(23): e2021JD035835

Jathar S H, Gordon T D, Hennigan C J, Pye H O, Pouliot G, Adams P J, Donahue N M, Robinson A L (2014). Unspeciated organic emissions from combustion sources and their influence on the secondary organic aerosol budget in the United States. Proceedings of the National Academy of Sciences of the United States of America, 111(29): 10473–10478

Laszakovits J R, Mackay A A (2022). Data-based chemical class regions for van krevelen diagrams. Journal of the American Society for Mass Spectrometry, 33(1): 198–202

Li L, Li J, Qin M, Xie X, Hu J, Zhang Y (2024). Variations in summertime ozone in Nanjing between 2015 and 2020: roles of meteorology, radical chain length and ozone production efficiency. Frontiers of Environmental Science & Engineering, 18(11): 137 doi.org/10.1007/s11783-024-1897-z

Li L, Ping T, Nakao S, Cocker D R III (2016). Impact of molecular structure on secondary organic aerosol formation from aromatic hydrocarbon photooxidation under low-NO_x conditions. Atmospheric Chemistry and Physics, 16(17): 10793–10808

Liu P, Wu Y, Li Z, Lv Z, Zhang J, Liu Y, Song A, Wang T, Wu L, Mao H, et al. (2024). Tailpipe volatile organic compounds (VOCs) emissions from Chinese gasoline vehicles under different vehicle standards, fuel types, and driving conditions. Atmospheric Environment, 323: 120348

Liu T, Wang Z, Huang D D, Wang X, Chan C K (2018). Significant production of secondary organic aerosol from emissions of heated cooking oils. Environmental Science & Technology Letters, 5(1): 32–37

Loza C L, Craven J S, Yee L D, Coggon M M, Schwantes R H, Shiraiwa M, Zhang X, Schilling K A, Ng N L, Canagaratna M R, et al. (2014). Secondary organic aerosol yields of 12-carbon alkanes. Atmospheric Chemistry and Physics, 14(3): 1423–1439

Lu Q, Zhao Y, Robinson A L (2018). Comprehensive organic emission profiles for gasoline, diesel, and gas-turbine engines including intermediate and semi-volatile organic compound emissions. Atmospheric Chemistry and Physics, 18(23): 17637–17654

Mader B T, Pankow J F (2001). Gas/solid partitioning of semivolatile organic compounds (SOCs) to air filters. 3. An analysis of gas adsorption artifacts in measurements of atmospheric SOCs and organic carbon (OC) when using Teflon membrane filters and quartz fiber filters. Environmental Science & Technology, 35(17): 3422–3432

Matsumoto K, Hayano T, Uematsu M (2003). Positive artifact in the measurement of particulate carbonaceous substances using an ambient carbon particulate monitor. Atmospheric Environment, 37(33): 4713–4717

Mcdonald B C, De Gouw J A, Gilman J B, Jathar S H, Akherati A, Cappa C D, Jimenez J L, Lee-Taylor J, Hayes P L, Mckeen S A, et al. (2018). Volatile chemical products emerging as largest petrochemical source of urban organic emissions. Science, 359(6377): 760–764

Peng J, Hu M, Du Z, Wang Y, Zheng J, Zhang W, Yang Y, Qin Y, Zheng R, Xiao Y, et al. (2017). Gasoline aromatics: a critical determinant of urban secondary organic aerosol formation. Atmospheric Chemistry and Physics, 17(17): 10743–10752

Peng J, Hu M, Shang D, Wu Z, Du Z, Tan T, Wang Y, Zhang F, Zhang R (2021). Explosive secondary aerosol formation during severe haze in the North China Plain. Environmental Science & Technology, 55(4): 2189–2207

Presto A A, Miracolo M A, Kroll J H, Worsnop D R, Robinson A L, Donahue N M (2009). Intermediate-volatility organic compounds: a potential source of ambient oxidized organic aerosol. Environmental Science & Technology, 43(13): 4744–4749

Qi L, Zhao J, Li Q, Su S, Lai Y, Deng F, Man H, Wang X, Shen X E, Lin Y, et al. (2021). Primary organic gas emissions from gasoline vehicles in China: Factors, composition and trends. Environmental Pollution, 290: 117984

Qiao L, Gao L, Liu Y, Huang D, Li D, Zheng M (2022). Recognition and health impacts of organic pollutants with significantly different proportions in the gas phase and size-fractionated particulate phase in ambient air. Environmental Science & Technology, 56(11): 7153–7162

Robinson A L, Donahue N M, Shrivastava M K, Weitkamp E A, Sage A M, Grieshop A P, Lane T E, Pierce J R, Pandis S N (2007). Rethinking organic aerosols: semivolatile emissions and photochemical aging. Science, 315(5816): 1259–1262

Shrivastava M, Cappa C D, Fan J, Goldstein A H, Guenther A B, Jimenez J L, Kuang C, Laskin A, Martin S T, Ng N L, et al. (2017). Recent advances in understanding secondary organic aerosol: Implications for global climate forcing. Reviews of Geophysics, 55(2): 509–559

Song K, Guo S, Gong Y, Lv D, Wan Z, Zhang Y, Fu Z, Hu K, Lu S (2023a). Non-target scanning of organics from cooking emissions using comprehensive two-dimensional gas chromatography-mass spectrometer (GC×GC-MS). Applied Geochemistry, 151: 105601

Song K, Guo S, Gong Y, Lv D, Zhang Y, Wan Z, Li T, Zhu W, Wang H, Yu Y, et al. (2022). Impact of cooking style and oil on semi-volatile and intermediate volatility organic compound emissions from Chinese domestic cooking. Atmospheric Chemistry and Physics, 22(15): 9827–9841

Song K, Tang R, Zhang J, Wan Z, Zhang Y, Hu K, Gong Y, Lv D, Lu S, Tan Y, et al. (2023b). Molecular fingerprints and health risks of smoke from home-use incense burning. Atmospheric Chemistry and Physics, 23(21): 13585–13595

Stewart G J, Acton W J F, Nelson B S, Vaughan A R, Hopkins J R, Arya R, Mondal A, Jangirh R, Ahlawat S, Yadav L, et al. (2021). Emissions of non-methane volatile organic compounds from combustion of domestic fuels in Delhi, India. Atmospheric Chemistry and Physics, 21(4): 2383–2406

Tang R, Lu Q, Guo S, Wang H, Song K, Yu Y, Tan R, Liu K, Shen R, Chen S, et al. (2021). Measurement report: distinct emissions and volatility distribution of intermediate-volatility organic compounds from on-road Chinese gasoline vehicles: implication of high secondary organic aerosol formation potential. Atmospheric Chemistry and Physics, 21(4): 2569–2583

Wagner T, Wyszyński M L (1996). Aldehydes and ketones in engine exhaust emissions: a review. Proceedings of the Institution of Mechanical Engineers. Part D, Journal of Automobile Engineering, 210(2): 109–122

Wu Y, Fan X, Liu Y, Zhang J, Wang H, Sun L, Fang T, Mao H, Hu J, Wu L, et al. (2023a). Source apportionment of VOCs based on photochemical loss in summer at a suburban site in Beijing. Atmospheric Environment, 293: 119459

Wu Y, Liu Y, Liu P, Sun L, Song P, Peng J, Li R, Wei N, Wu L, Wang T, et al. (2023b). Evaluating vehicular exhaust and evaporative emissions via VOC measurement in an underground parking garage. Environmental Pollution, 333: 122022

Zeng L, Wang F, Xiao S, Zeng X, Li X, Xie Q, Yu X, Huang C, Hu Q, You Y, et al. (2024). Characterization and prediction of tailpipe ammonia emissions from in-use China 5/6 light-duty gasoline vehicles. Frontiers of Environmental Science & Engineering, 18(1): 6

Zhang J, Peng J, Song A, Du Z, Guo J, Liu Y, Yang Y, Wu L, Wang

T, Song K, et al. (2024a). Secondary organic aerosol formation potential from vehicular non-tailpipe emissions under real-world driving conditions. Environmental Science & Technology, 58(12): 5419–5429

Zhang J, Peng J, Song A, Lv Z, Tong H, Du Z, Guo J, Wu L, Wang T, Hallquist M, et al. (2023).Marked impacts of transient conditions on potential secondary organic aerosol production during rapid oxidation of gasoline exhausts. npj Climate and Atmospheric Science, 6(1): 59

Zhang X, He X, Cao Y, Chen T, Zheng X, Zhang S, Wu Y (2024b). Comprehensive characterization of speciated volatile organic compounds (VOCs), gas-phase and particle-phase intermediate- and semi-volatile volatility organic compounds (I/S-VOCs) from Chinese diesel trucks. Science of the Total Environment, 912: 168950

Zhang Y, Wang X, Wen S, Herrmann H, Yang W, Huang X, Zhang Z, Huang Z, He Q, George C (2016). On-road vehicle emissions of glyoxal and methylglyoxal from tunnel tests in urban Guangzhou, China. Atmospheric Environment, 127: 55–60

Zhao B, Wang S, Hao J (2024). Challenges and perspectives of air pollution control in China. Frontiers of Environmental Science & Engineering, 18(6): 68

Zhao J, Lv Z, Qi L, Zhao B, Deng F, Chang X, Wang X, Luo Z, Zhang Z, Xu H, et al. (2022). Comprehensive assessment for the impacts of S/IVOC emissions from mobile sources on SOA formation in China. Environmental Science & Technology, 56(23): 16695–16706

Zhao Y, Hennigan C J, May A A, Tkacik D S, De Gouw J A, Gilman J B, Kuster W C, Borbon A, Robinson A L (2014). Intermediate-volatility organic compounds: a large source of secondary organic aerosol. Environmental Science & Technology, 48(23): 13743–13750

Zhao Y, Lambe A T, Saleh R, Saliba G, Robinson A L (2018). Secondary organic aerosol production from gasoline vehicle exhaust: effects of engine technology, cold start, and emission certification standard. Environmental Science & Technology, 52(3): 1253–1261

Zhao Y, Nguyen N T, Presto A A, Hennigan C J, May A A, Robinson A L (2015). Intermediate volatility organic compound emissions from on-road diesel vehicles: chemical composition, emission factors, and estimated secondary organic aerosol production. Environmental Science & Technology, 49(19): 11516–11526

Zhao Y, Nguyen N T, Presto A A, Hennigan C J, May A A, Robinson A L (2016). Intermediate volatility organic compound emissions from on-road gasoline vehicles and small off-road gasoline engines. Environmental Science & Technology, 50(8): 4554–4563